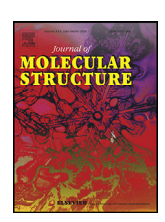
ELSEVIER

Contents lists available at ScienceDirect

Journal of Molecular Structure

journal homepage: www.elsevier.com/locate/molstr



Co-crystals of polynuclear aromatic hydrocarbons and 9H-carbazole with 2,3-dichloro-5,6-dicyano-1,4-benzoquinone acceptor: Varieties in crystal packing, Hirshfeld surface analysis and quantum-chemical studies



Marina S. Fonari a,b, Sergei Rigin a,*, Daniel Lesse a, Tatiana V. Timofeeva a

ARTICLE INFO

Article history: Received 21 June 2022 Revised 20 December 2022 Accepted 31 December 2022 Available online 2 January 2023

Keywords:
X-ray diffraction
Donor-acceptor co-crystals
Charge transfer
Polynuclear aromatic hydrocarbons (PAH)
2,3-dichloro-5,6-dicyano-1,4-benzoquinone (DDO)

ABSTRACT

Co-crystals formed by polynuclear aromatic hydrocarbons (PAH) chrysene, benz(a)anthracene, triphenylene(9,10-benzophenanthrene), benzo(a)pyrene, dibenz[a,c]anthracene, and 9H-carbazole as π -electron-donor (D) molecules, with π -electron acceptor, 2,3-dichloro-5,6-dicyano-1,4-benzoquinone (DDQ) were synthesized, and their crystal structures were determined using single-crystal X-ray diffraction analysis. All co-crystals exhibit 1:1 donor / acceptor ratio and adopt mixed-stacking motifs. The donor(D)-acceptor (DDQ) π - π interactions in stacks are complemented by different sets of D···D, D···DDQ and DDQ···DDQ intermolecular interactions between stacks whose diversity originates from different degree of D/DDQ mismatch and manifests in dissimilar crystal packing motifs. The parallel face-to-face stacking was registered in chrysene-DDQ, while benz(a)anthracene-DDQ reveals brickwork crystal packing with significant parallel slippage. The rest four co-crystals show fairly different herringbone-type crystal packing with rearrangement of intermolecular interactions. The distribution of intermolecular contacts and impact of π - π interactions were evaluated through Hirshfeld surface analysis. Molecular orbital energies as well as bandgaps were calculated using DFT. Degree of charge-transfer was estimated based on bond length distribution in the acceptor molecule for each of the co-crystals.

© 2023 Elsevier B.V. All rights reserved.

1. Introduction

Discovery of a highly conducting tetrathiafulvalene (TTF) – tetracyano-p-quinodimethane (TCNQ) complex [1,2], initiated tremendous attention towards charge-transfer (CT) organic solids that include π -electron donors (D) and another component as a π -electron acceptor (A), that both are typically planar molecules presenting packing mode enabling CT interactions in the solid state. These two-component organic donor–acceptor CT co-crystals based on p-A pairs with typical mixed or segregated stack motif, generally display unique crystalline structures and superior optoelectronic properties in the solid state and remain in focus of contemporary demands for new efficient organic semiconductors (OSC) regard to their applications in organic field-effect transistors (OFETs) [3–5].

Typically, ambipolar charge transport is generated by co-assembling of p- and n-type semiconductors. For twocomponent co-crystal ambipolar transport behavior was first registered for (BEDT-TTF)(F₂-TCNQ) (BEDT-TTF=bis(ethylenedithio) tetrathiafulvalene) [6] and DA co-crystals with both electron [6] and hole field-effect mobilities exceeding $0.1 \text{ cm}^2\text{V}^{-1}\text{s}^{-1}$ were documented [7,8]. Furthermore, an exceptional example, the single crystal device based on complex DPTTA-F2TCNQ (DPTTA=mesodiphenyl tetrathia[22]annulene[2,1,2,1]; F₂-TCNQ=2,5-difluoro-7,7,8,8-tetracyanoquinodimethane) reveals the hole and the charge-carrier mobilities up to $1.57~{\rm cm^2}~V^{-1}~s^{-1}$ for holes and 0.47 cm² V - 1 s - 1 for electrons [8]. The influence of packing modes and D-A interactions on the transport properties was also discussed through the combination of experimental and theoretical studies and recent theoretical studies show that high ambipolar semiconductor behavior is a result of synergism between two main charge carrier transfer pathways in cocrystal system viz. superexchange via mixed DADADA stacks and direct paths of charge carriers, as via DD dimeric pairs [9,10].

^a New Mexico Highlands University, Las Vegas 87701, NM, United States

b Institute of Applied Physics, Academy Str., 5 MD2028, Chisinau, Moldova

^{*} Corresponding author.

E-mail address: rigindale@gmail.com (S. Rigin).

Fig. 1. Structural formulas for (a) DDQ acceptor and PAH donors (b) chrysene; (c) benzo(a)anthracene; (d) triphenylene; (e) benzo(a)pyrene; (f) dibenz[a,c]anthracene; (g) 9H-carbazole.

However, electronic performance of CT materials is still difficult to predict and control, since same donor and acceptor molecules can yield crystals with different packing (polymorphs) and stoichiometry [11–14]. For instance, an unusual mixed stacked packing arrangement was documented for the system dithieno[3,2-a:2',3'-c]phenazine (DTPhz)-TCNQ (2:1 D:A ratio) accompanied by stronger electronic interactions orthogonal to stacks and originated from edge-to-edge D-D and A-A contacts [15]. When developing CT organic materials, crystal engineering is useful to explore the relation between crystal packing and charge carrier polarity and to analyze the supramolecular networks and intermolecular interactions as the channels for electron and hole transport [16–21].

Since the conducting salt, TTF-DDQ (DDQ=2,3-dichloro-5,6dicyanobenzoquinone) composed of strongly distorted stacks of DDQ and isolated eclipsed dimers of TTF was reported [22,23], DDQ and its analogues are widely exploited as powerful acceptors for crystal engineering of potential CT materials with meaningful conducting properties [21-36]. For example, formation of solid solutions between isomorphous CT co-crystals with variable DDQ;DBQ (DBQ=2,3-dibromo-5,6-dicyanobenzoquinone) molar ratio was suggested to predictably tune degree of charge transfer of solids because the packing motif remained unaffected by compositional changes [33]. On the other hand, reported by the other group the salts of DDQ radical with substituted N-ethyl- and Nmethylpyridinium cations represent either structures with stacks of equidistant radicals (interplanar separation < 3.3 A) being fairly good semiconductors, or Peierls-distorted stacks comprising diamagnetic dimers of radicals (interplanar separations are < 3.1 A within the dimers and > 3.4 A between the dimers) being insula-

Polyaromatic hydrocarbons (PAHs) proved their efficacy as suitable donors in mixed-stacked co-crystals [5,26-28,30-32,36-38] and exhibit excellent intrinsic charge transport properties. However, very few co-crystals of DDQ with PAHs were reported so far [30,31,36,39] that explains our present research. The structural formulas for DDQ acceptor and donor molecules considered in this study are shown in Fig. 1.

As a rule, charge-transfer is possible if the energy gaps between the highest occupied molecular orbital (HOMO) of donor and the lowest unoccupied molecular orbital (LUMO) of acceptor overlap. In other words, HOMO level of donor molecule should have a lower energy than LUMO level of acceptor. The preliminary quantum-chemical calculations were fulfilled to evaluate D/A HOMO/LUMO

orbitals as the requirement for CT complex formation and six CT complexes were synthesised by combination of these components and their crystal structures are discussed in detail. Crystal structures were investigated using single crystal X-Ray diffraction analysis. All quantum chemical calculations were carried out using GAUSSIAN 16 software [40].

2. Results and discussion

2.1. Quantum chemical calculations for PAH donors and common acceptors

As acceptors for quantum-chemical calculations three common TCNQ, PMDA and DDQ acceptors have been chosen. For these acceptors 875, 87 and 106 structures of co-crystals respectively have been found in CSD (CSD version 5.43 updates Sept. 2022). For TCNQ co-crystals with about 20 PAHs, for PMDA with about 10 PAHs and with DDQ with only 2 PAHs have been described in the literature (Table 2S). In our search we considered only polyaromatic hydrocarbon molecules which are built with only 6membered aromatic rings not containing substituents and heteroatoms with one exception of 9H-carbazole. Quantum chemical calculations that include calculation of the energy levels and HOMO-LUMO gaps for the potential components were performed and the results are graphically illustrated in Fig. 2, Fig. S1 and Tables 1 and 2. Fig. S1 depicts the shapes of HOMO and LUMO orbitals, corresponding to the energy values presented in Tables 1 and 2. It should be noted that the molecular geometry, the energy values and the shape of the orbitals were calculated for isolated molecules, but when these molecules form a crystal, their geometry can change leading to different shape of the orbitals and corresponding energy values. Thus, calculated energies of HOMO and LUMO levels are approximate and should be used only for estimation purposes. As seen from Fig. 2, all aromatic donors have a HOMO-LUMO bandgap overlap with all the proposed acceptors. For further studies under this project, we choose one acceptor DDQ, since only two co-crystals of this acceptor with PAHs have been described in the literature till now. The lowest HOMO level was observed for triphenylene (-6.2 eV). It also has the widest bandgap among donors (4.84 eV). Several donor-acceptor pairs were chosen for co-crystallization based on quantum computation results. Various crystal growth techniques such as slow evaporation and vapor diffusion were used to obtain desired co-crystals.

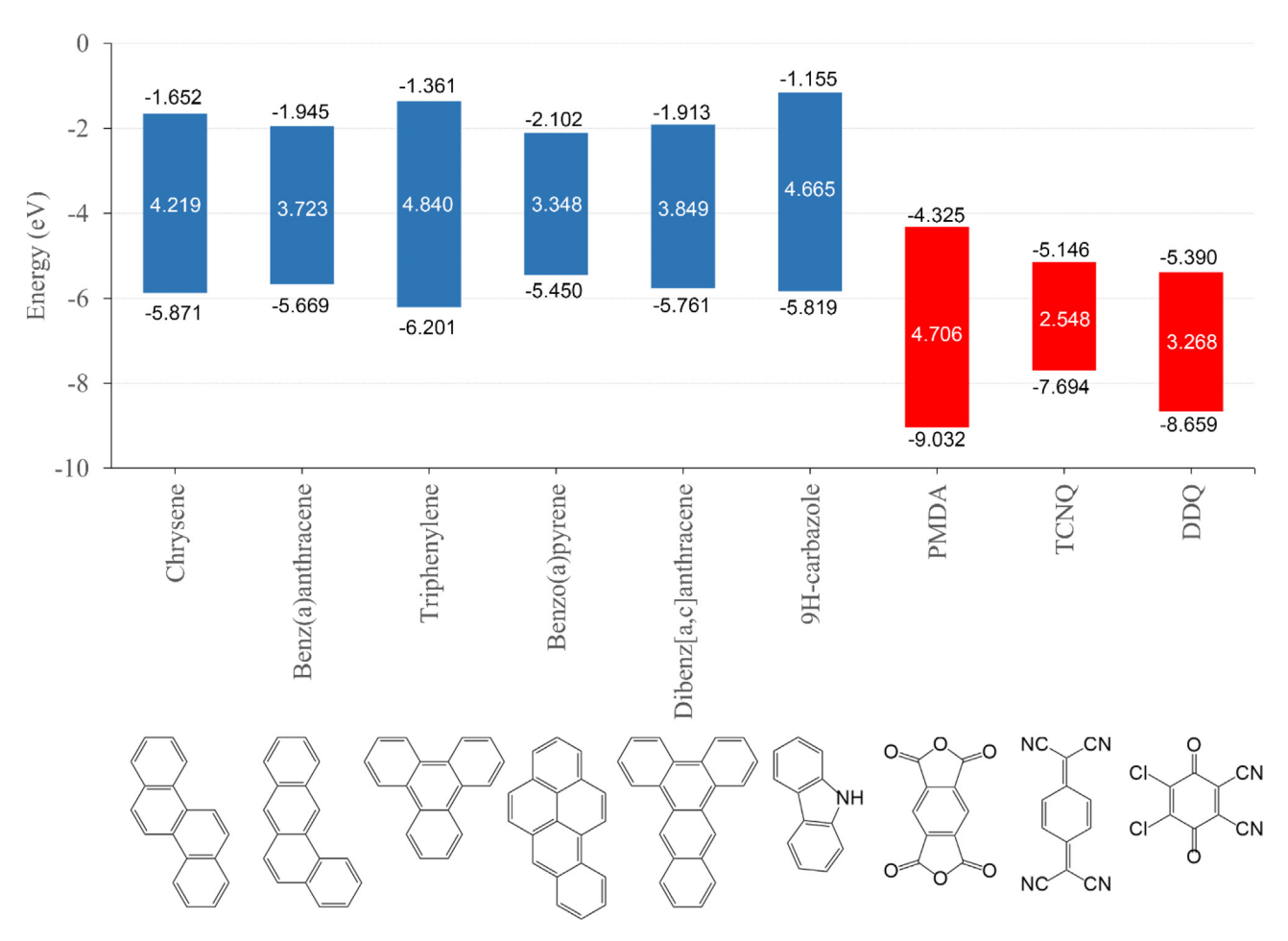


Fig. 2. Calculated energy levels and energy differences between HOMO and LUMO levels for PAH donors (blue) and common acceptors (red).

Table 1 Calculated energy (eV) values for aromatic donors.

Energy, eV	Chrysene	Benz(a)anthracene	Triphenylene	Benzo(a)pyrene	Dibenz[a,c]anthracene	9H-carbazole
E _{HOMO}	-5.871	-5.669	-6.201	-5.450	-5.761	-5.819
E_{LUMO}	-1.652	-1.945	-1.361	-2.102	-1.913	-1.155
ΔE	4.219	3.723	4.840	3.348	3.849	4.665

 Table 2

 Calculated energy (eV) values for common acceptors.

Energy, eV	PMDA	TCNQ	DDQ
E _{HOMO}	-9.032	-7.694	-8.659
E _{LUMO}	-4.325	-5.146	-5.390
ΔE	4.706	2.548	3.268

2.2. Synthesis and structure of co-crystals

All co-crystals were obtained similarly by the vapor diffusion technique. Equimolar saturated solutions of components in chloroform were prepared in separate containers. Saturated solutions were mixed and stirred for 15 min. Resulting solution was filtered using syringe filter. Filtered solution was placed in growth chamber of diffusion vessel with pentane as a secondary solvent. Images for the selected crystals are shown in Fig. 3. All co-crystals have needle-like shapes and are colored differently than either one of the pure components, indicating possible electronic interaction between the donor (D) and DDQ molecules in the co-crystal phases. The crystallographic data are summarized in Table 3.

2.3. Crystal packing

All co-crystals reveal 1:1 D:DDQ ratio. Co-crystals chrysene-DDQ, benz(a)anthracene-DDQ, and triphenylene-DDQ are isoelectronic, and have the same C/H ratio (1.5) for donors, which varies for benzo(a)pyrene (1.667), and dibenz[a,c]anthracene (1.571). The asymmetric unit of the monoclinic co-crystal triphenylene-DDQ comprises two formula units, D1-DDQ1 and D2-DDQ2, while all the rest co-crystals contain one D-DDQ pair of molecules per asymmetric unit.

The ORTEP diagrams for co-crystals with atomic numbering schemes are given in Fig. S2. In the co-crystal benz(a)pyrene-DDQ the DDQ molecule is disordered by rotation of 180° about the central O = C...C = O axis with 60% to 40% ratio between disordered components (Fig. S2). This type of disorder was registered for DDQ molecule in co-crystals of TTF-DDQ [23] and BEDT-TTF-DDQ [41]. The rotation disorder was also registered for 9H-carbazole donor in 9H-carbazole-DDQ co-crystal. All molecules possess flat skeletons with insignificant deviations from planarity. Everywhere the primarily packing motif is a 1D mixed-stack with the almost parallel arrangement of the molecules in stacks as indicate interplanar D/DDQ angles (range 2–4°) summarized in Table S1. In stacks

Table 3Crystal data and structure refinement parameters for co-crystals.

	Chrysene-DDQ	Benz(a)anthracene-DDQ	Triphenylene-DDQ	Benz(a)pyrene-DDQ	Dibenz[<i>a</i> , <i>c</i>] anthracene-DDQ	9H-carbazole-DDQ
Empirical formula	C ₂₆ H ₁₂ Cl ₂ N ₂ O ₂	C ₂₆ H ₁₂ Cl ₂ N ₂ O ₂	C ₂₆ H ₁₂ Cl ₂ N ₂ O ₂	C ₂₈ H ₁₂ Cl ₂ N ₂ O ₂	C ₃₀ H ₁₄ Cl ₂ N ₂ O ₂	C ₂₀ H ₉ Cl ₂ N ₃ O ₂
Formula weight	455.28	455.28	455.28	479.30	505.33	394.20
Temperature, K	150(2)	300(2)	150(2)	100(2)	100(2)	173(2)
Crystal size, mm ³	$0.50\times0.35\times0.08$	$0.115 \times 0.111 \times 0.109$	$0.35\times0.25\times0.05$	$0.31\times0.20\times0.07$	$0.55\times0.18\times0.08$	$0.70\times0.12\times0.12$
Crystal system	Triclinic	Monoclinic	Monoclinic	Orthorhombic	Monoclinic	Monoclinic
Space group	P-1	$P2_1/n$	$P2_1/n$	P2 ₁ 2 ₁ 2 ₁	P2 ₁ /c	$P2_1/n$
a, Å	6.997(6)	8.522(2)	7.094(4)	7.043(6)	14.8(2)	7.052(3)
b, Å	11.407(10)	15.013(4)	30.935(18)	8.150(7)	8.42(12)	9.140(6)
c, Å	12.774(11)	16.495(4)	18.168(11)	35.78(3)	17.9(3)	25.891(15)
α,°	96.878(10)	90	90	90	90	90
β,°	93.727(10)	102.863(4)	90.594(8)	90	93.72(9)	93.338(16)
γ, °	106.354(10)	90	90	90	90	90
Volume, Å ³	966.0(14)	2057.4(9)	3987(4)	2053(3)	2226(57)	1666.0(16)
Z	2	4	8	4	4	4
$D(_{\rm calcd})$, g/cm ³	1.565	1.470	1.517	1.550	1.508	1.572
μ , mm $^{ ext{-}1}$	0.366	0.343	0.354	0.349	0.326	0.412
F(000)	464	928	1856	976	1032	800
Reflections collected/	14,179	26,500	81,601	36,914	25,557	26,764
Data / restraints / parameters	3387 0 290	6077 0 289	7037 0 578	3626 / 0 / 237	3917 / 0 / 325	3274 466 313
Final R indices $[I>2\sigma(I)]$, R_1 , wR_2	0.1142, 0.3078	0.0481, 0.1205	0.0894, 0.1718	0.1037, 0.2689	0.1082, 0.2301	0.0612, 0.1390
R indices (all data), R_1 , wR_2	0.1558, 0.3243	0.0804, 0.1394	0.2628, 0.2235	0.2071, 0.3225	0.3855, 0.3376	0.0838, 0.1466

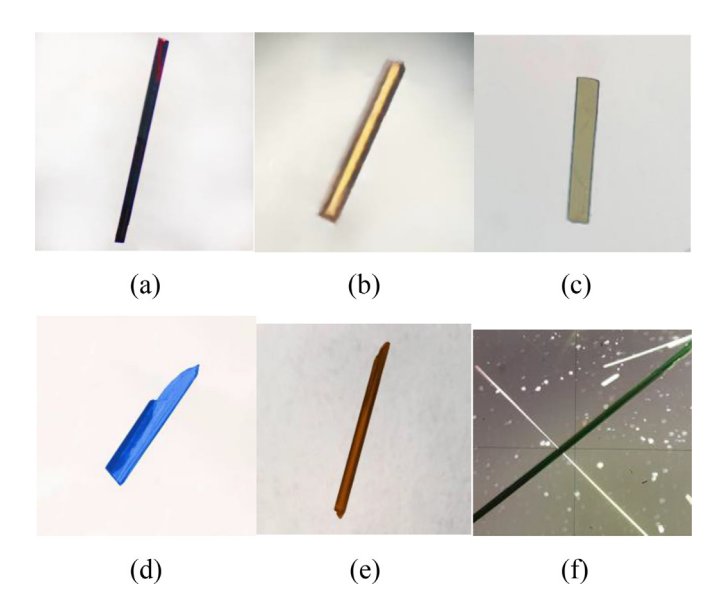


Fig. 3. Images of co-crystals (a) chrysene-DDQ; (b) benz(a)anthracene-DDQ; (c) triphenylene-DDQ; (d) benzo(a)pyrene-DDQ; (e) dibenz[a,c]anthracene-DDQ; (f) 9H-carbazole-DDQ.

the DDQ acceptor is situated approximately equidistant between two successive donor molecules with different D/DDQ contact areas as it is evidenced from Fig. 4 and indicated by the meaningful centroid "centroid (Cg(D)" $Cg(DDQ) \angle 4 \text{ Å}$) distances between overlapping six-membered rings (Table S1). Two chrysene donor molecules ideally cover each DDQ molecule, while in the rest of co-crystals the overlapping domains vary significantly revealing different degrees of D/DDQ mismatch. In 9H-carbazole-DDQ cocrystal the C = O groups of DDQ fail to stack over the rings of donor, in all other structures the DDQ C = 0 groups are superposed on the rings of one (or two) donor molecules to give rise to dipole-induced forces contribution in overall system of D-DDQ interactions. The significant slippage with the smaller contact area is demonstrated for the benz(a)anthracene-DDQ co-crystal and is manifested by the lack of Cg(DDQ)···Cg(D) meaningful interaction for the translated along the stack second benz(a)anthracene donor molecule (Table S1).

Although all co-crystals display a "typical" mixed stack (DADA) pattern where donor sits directly atop an acceptor which maximizes D/DDQ π - π -interactions, packing of stacks reveals different packing motifs originated from different donors' molecular shapes and C/H ratios and manifested in different sets of the edge-to-edge and edge-to-face intermolecular contacts.

In the triclinic co-crystal chrysene–DDQ mixed stacks run along the shortest *a* axis (Fig. 5a) and are packed in a parallel mode. Molecules from adjacent stacks form slightly corrugated layers that are tilted relative to the stack axis by 70.17° In the layer the rows of chrysene and DDQ molecules alternate and are interconnected via edge-to-edge chrysene-chrysene [42,43], chrysene-DDQ, and DDQ-DDQ short contacts summarized in Table S1. Adjacent DDQ molecules in layer are interconnected by two symmetrical Cl···O bonds (3.209(3) Å) forming a centrosymmetric dimer.

Similar to the previous structure in the monoclinic co-crystal benz(a)anthracene-DDQ mixed stacks are also packed in a parallel mode. However, the structure reveals significant D/DDQ slippage resulted in a brickwork packing arrangement because of the D/DDQ mismatch. It is the most loosely packed structure with the lowest crystal density (see Table 3). Molecules from adjacent stacks align in the layer that is tilted relative to the stack axis by 78.35 ° (Fig. 6). Although the layer's topology retains, the intermolecular contacts increase. The stabilizing remain two short donor-DDQ CH...O(N) interactions and CH···CH contacts (Table S1), while Cl···O distance increases up to 4.511 Å.

The monoclinic co-crystal triphenylene-DDQ is unique because of two formula units that are arranged in an angular mode indicated by D1/D2 and DDQ1/DDQ2 tilted angles of 47.50(6) and 42.60(5)°. Each formula unit forms its own (but alike) mixed stack, -D1-DDQ1-D1- and D2-DDQ2-D2-, both extending along the shortest crystallographic a axis. The stacks alternate along the longest b-axis. Parallel to the ac plane these two types of stacks form two different stacking layers. Adjacent stacks -D1-DDQ1-D1 symmetry related by inversion and translation are interconnected via lateral CH...N and CH...Cl contacts that combine molecules in coplanar chains with alternative arrangement of the molecules in chains. Thus, the stacking layer with parallel arrangement of molecules is reinforced by stacking interactions along the stacks and -D1-DDQ1-D1- short contacts across the stacks (Fig. 7a). In this stacking layer single face-to-face contact C(51)···C(51)(-x,1-y, -z)=3.315(12)Å was registered between donor molecules related by inversion.

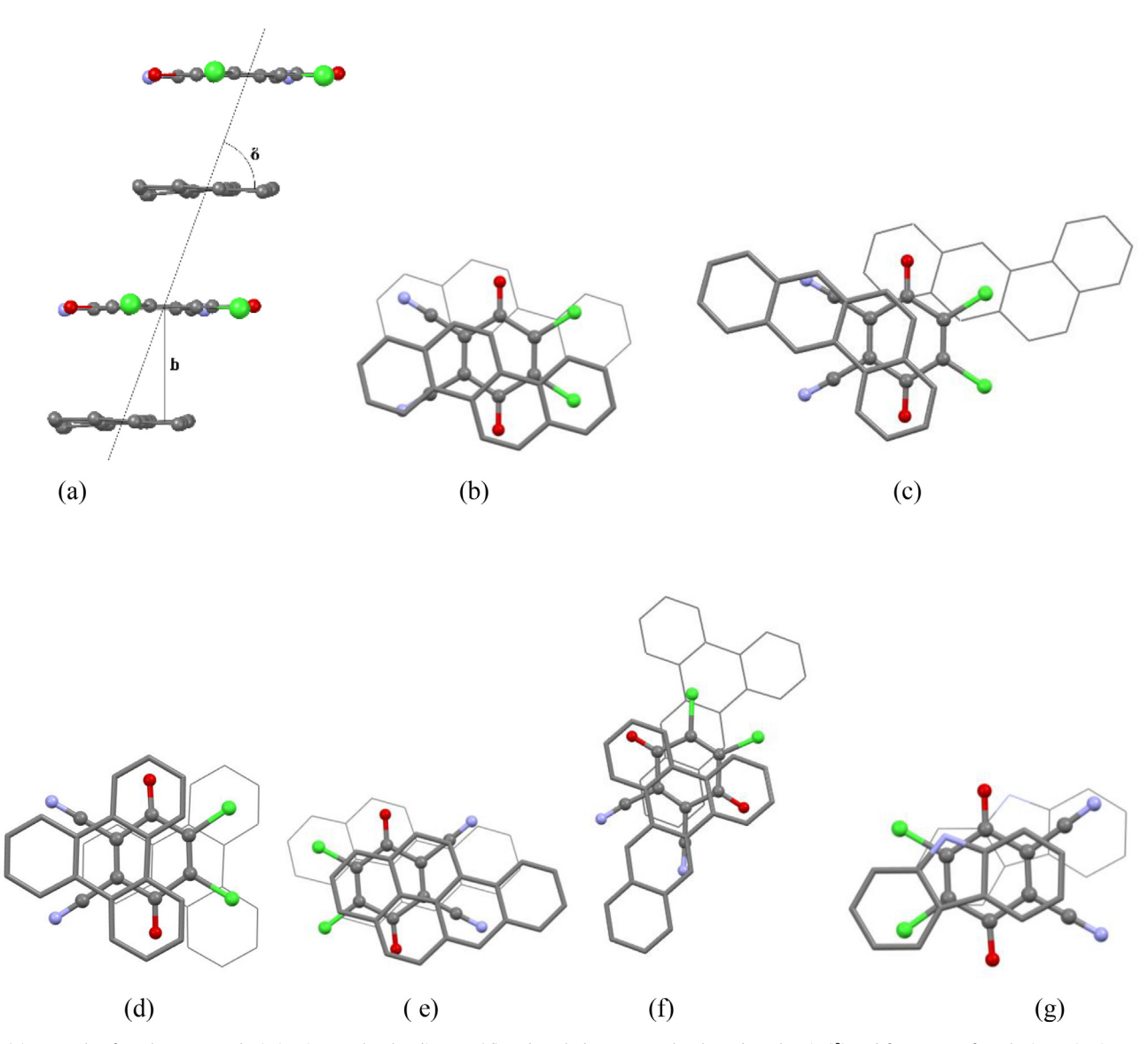


Fig. 4. (a). Example of **s**tack structure depicting intermolecular distance (**d**) and angle between molecule and stack axis (δ) and fragments of stacks in projection on DDQ molecule occupying middle positions between two donor molecules shown in stick and wireframe styles for co-crystals (b) chrysene-DDQ; (c) benzo(a)anthracene-DDQ; (d) triphenylene-DDQ; (e) benzo(a)pyrene-DDQ; (f) dibenz[a,c]anthracene-DDQ; (g) 9H-carbazole-DDQ.

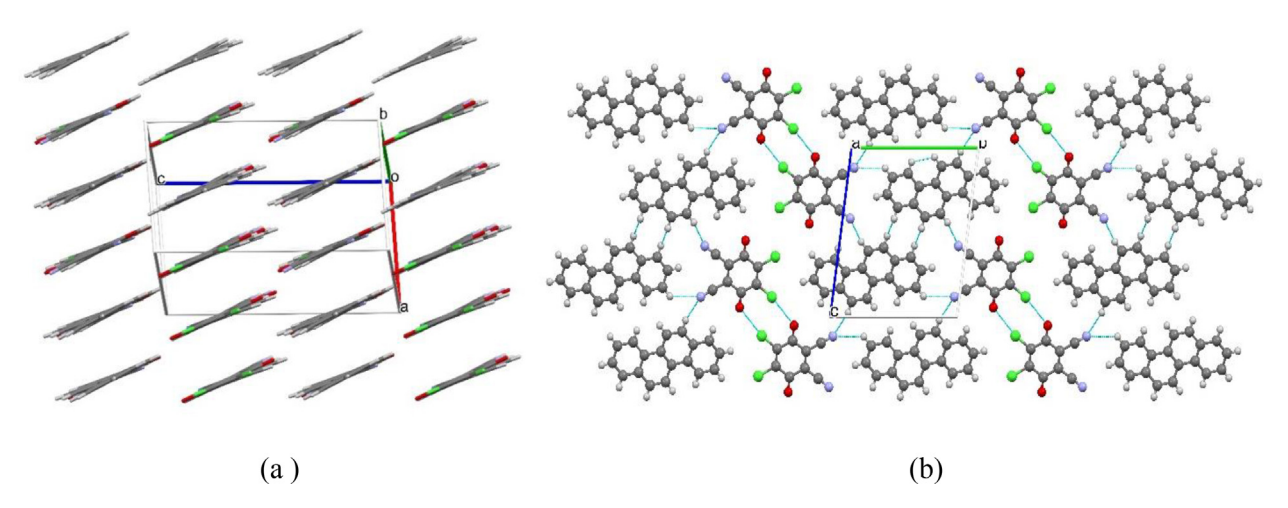


Fig. 5. Fragments of crystal packing in co-crystal chrysene-DDQ. (a) parallel 1D stacking; (b) layer motif in the bc plane.

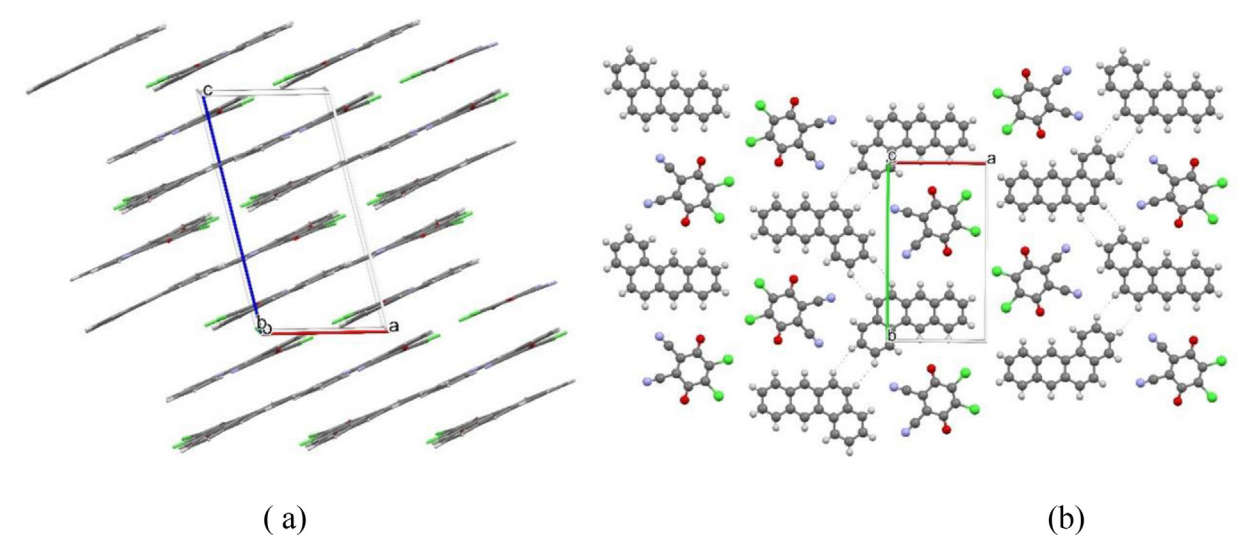


Fig. 6. Fragments of crystal packing in structure benz(a)anthracene-DDQ. (a) brickwork packing; (b) layer motif in the ab plane.

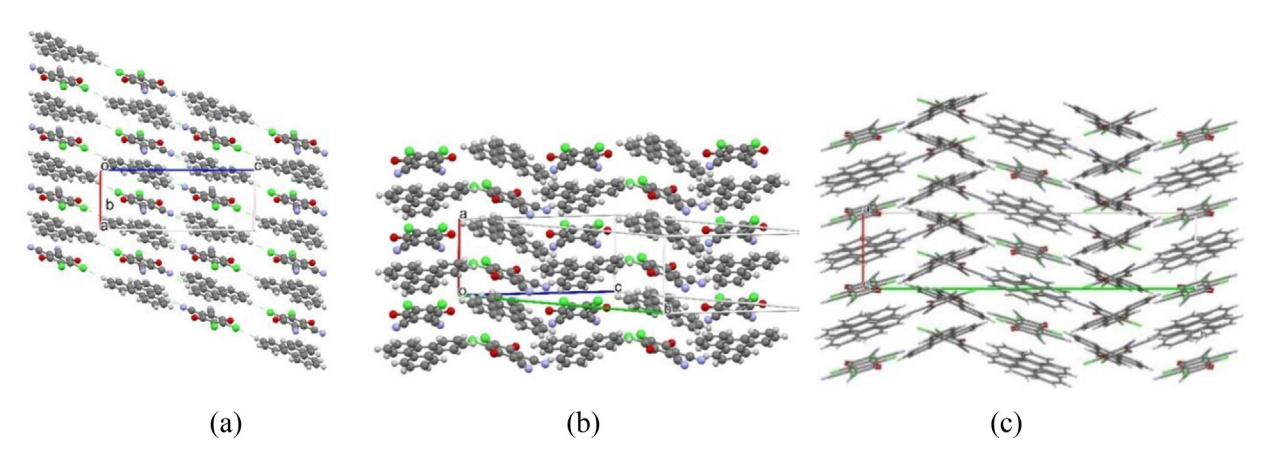


Fig. 7. Fragments of crystal packing in co-crystal triphenylene-DDQ; (a) stacking layer -D1-DDQ1-D1- with parallel arrangement of stacks; (b) stacking layer -D2-DDQ2-D2-with herring-bone arrangement of stacks; (c) interconnection of two stacking motifs.

Adjacent stacks -D2-DDQ2-D2- symmetry related by 2_1 axis pack in a herring-bone stacking layer with the D2/D2 and DDQ2/DDQ2 tilted angles of 46.03 and 40.39° (Fig. 7b). This arrangement is accompanied by disruption of part of the contacts registered in the chain -D1-DDQ1-D1- and instead rapprochement of D2 donor molecules interconnected via H···H short contact, H18···H29(x-1/2, 1/2-y, 1/2 + z)=2.368 Å giving rise to the D-D-D zigzag chain across this layer (Fig. S3a).

The combination of parallel and herring-bone 2D stacking motifs occurs via interplay of D1/DDQ2 and D2/DDQ1 edge-to edge contacts (Fig. 7c). This results in infinite donor-donor networks as interplay of D2-D2 zigzag chains and D1-D1 dimers (Fig. S3b).

Co-crystal benzo(a)pyrene-DDQ is unique since it is the only one compound in this series that crystallizes in the non-centrosymmetric orthorhombic space group $P2_12_12_1$. The mixed stacks run along the shortest a axis and molecules from adjacent stacks are interconnected in the H-bonded chains via CH···O and CH···N short contacts across the stacks (Table S1). Molecules in chain tilted relative to the stack axis by 70.23° These side contacts combine adjacent stacks in the stacking polar layers parallel to the ab plane with parallel arrangement of the molecules in the layers (Fig. 8a). The adjacent layers related by the 2_1 axes meet either by phenyl or pyrene residues (Fig. 8c). In the former case they are interconnected via edge-to-edge CH(D)···N(DDQ) and edge-to-face CH(D)···C(D) short contacts, the latter ones combine benz(a)pyrene

donor molecules in a herring-bone chain along the a axis with the tilted angle between neighboring benz(a)pyrene molecules of 39.6° (Fig. S3c). No short contacts less than sum of van der Waals radii were found between layers when they contact by pyrene moieties.

In the monoclinic co-crystal dibenzo[a,c]anthracene-DDQ alternation -D-DDQ-D- occurs in stacks along the b axis and molecules form ribbons along a axis where they are interlinked via two weak CH···N bonds (Table S1). These lateral interactions combine stacks in stacking layer parallel to the ab plane (Fig. 9a). The wave-like ribbons provide rapprochement of two adjacent donor molecules from neighboring stacks related by inversion and separated by 2.358 Å that provide their face-to-face short contacts of C(27)···C(12)(1-x,1-y,2-z)=3.38(6) Å. Along the c axis the layers meet in an edge(D,A)-to-face(D) T-shaped stacking mode (D/D angle is 77.90 °) through the short CH···C interactions. It is noteworthy, that dibenzo[a,c]anthracene donor forms its own 3D infinite network via CH...C and CH...CH short homomeric contacts (Fig. S3d)

The monoclinic co-crystal 9H-carbazole-DDQ is unique due to the presence of strong H-donor, NH-group in the donor molecule. That influences hierarchy of intermolecular interactions. Mixed stacks run along the shortest crystallographic *a* axis. The shortest NH···N(DDQ) interaction N(3A)-H3A···N(2)(*x*-1/2, 3/2-*y*, *z*-1/2) 2.29 Å was found between donor and acceptor related by the glide plane and it arranges adjacent stacks in herring-bone mode with

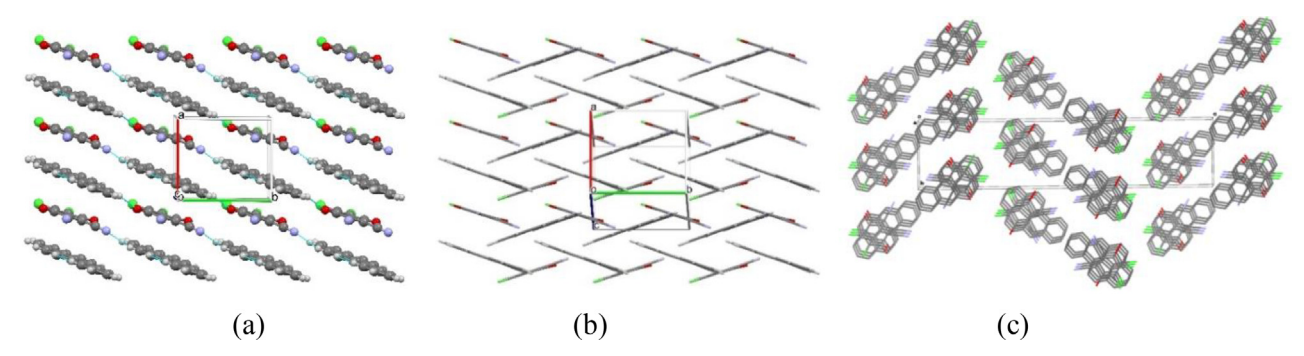


Fig. 8. Structure of benzo(a)pyrene-DDQ co-crystal: (a) view of a stacking layer, (b) herring-bone crystal packing; (c) crystal packing, view along a axis.

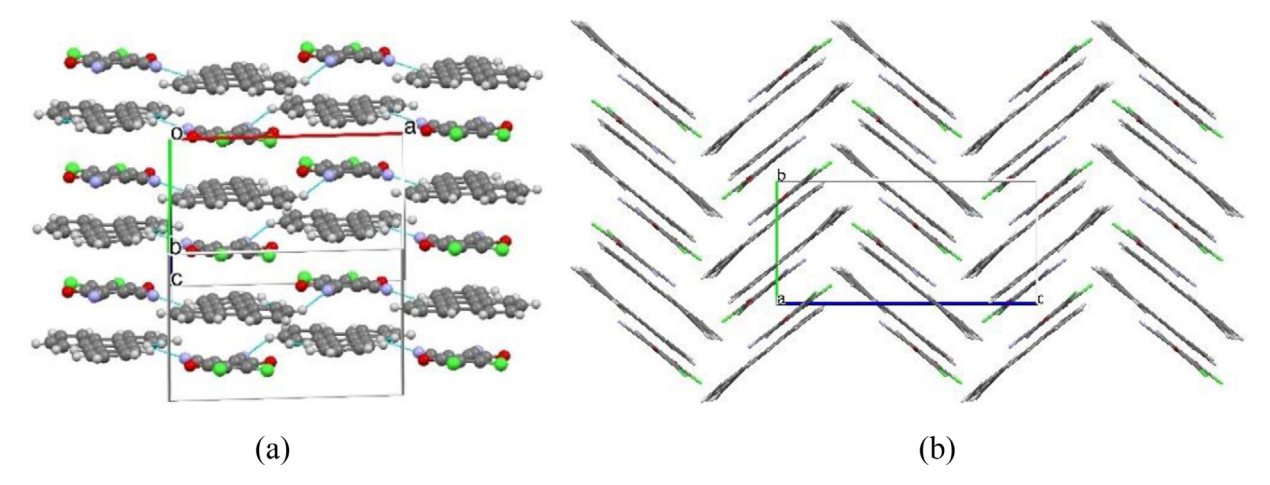


Fig. 9. Crystal structure of dibenzo[a,c]anthracene-DDQ co-crystal: (a) view of stacking layer (molecular planes are perpendicular to the layer), (b) crystal packing, view along a axis.

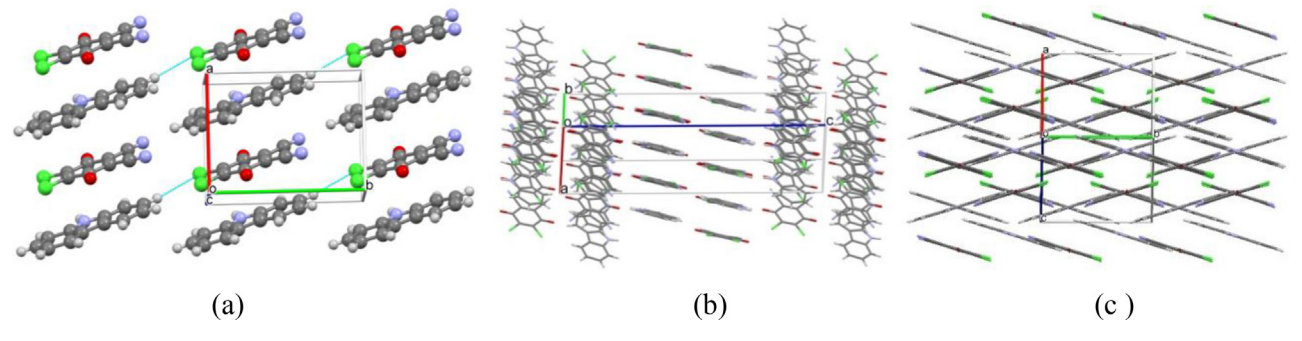


Fig. 10. Crystal structure of carbazole-DDQ co-crystal: (a) view of stacking layer, (b) interplay of parallel and herring-bone stacking modes (c) crystal packing.

the D/DDQ angle of 34.56 °. However, each four stacks translated along b axis and related by inversion, are combined in tetrads via two pairs of centrosymmetric CH···Cl and CH···N short contacts thus giving rise to the double stacking layer (Fig. 10a,b) with virtually parallel alignment of molecules within this layer of 11.32 Å thickness. These layers meet in an edge-to-face mode linked via abovementioned NH···N hydrogen bond and short Cl···O contact, Cl(2)···O(1)(1/2-x, y-1/2, 3/2-z)=3.154(3) Å, the latter one combining DDQ acceptors into helical chain with the DDQ/DDQ tilted angle of 34.43 °(Fig. S4). The same DDQ arrangement was registered in phenanthrene-DDQ co-crystal [31].

2.4. Hirshfeld surface analysis

Hirshfeld surface analysis [44,45] enables the quantitative description of intermolecular interactions occurring within the crystal lattice. For this purpose, the normalized contact distance (d_{norm})

feature of the computed Hirshfeld surface, based on the internal (di) and external (de) distances, was employed. The corresponding 3D maps of the Hirshfeld surfaces, where d_{norm} is visualized, for all co-crystals are shown in Fig. 11. The regions with an intense red color are located over the oxygen and the nitrogen atoms. These spots are attributed to the hydrogen bonds in which these atoms participate.

Table 4 and Fig. S5 summarize the most meaningful interactions in all structures. The analysis of the 2D fingerprint plots of the Hirshfeld surfaces reveals that redistribution of weak interactions from structure to structure occurs in narrow intervals, and the meaningful remain H···H, H···N, H···Cl and H···O interactions given in a descending order. The H···N hydrogen bonds giving an impact of 16.8%–21.6%, manifest as two sharp, symmetric spikes in all but dibenz[a,c]anthracene-DDQ co-crystal where they are significantly masked by excessive H···H contacts. Other meaningful are H···H donor-donor interactions that comprise 15.4–22.6%,

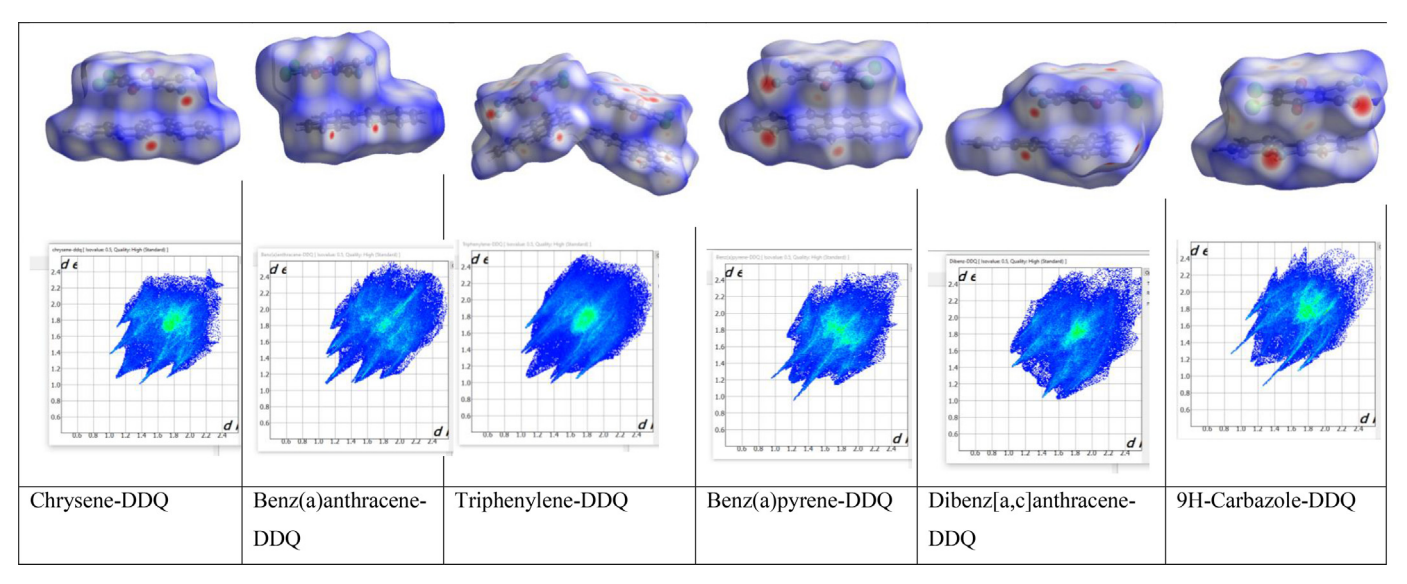


Fig. 11. Hirshfeld surfaces and overall 2D plots for studied co-crystals.

Table 4Distribution of meaningful contacts (%) in reported structures based on Hirshfeld surface analysis.

Co-crystal	Н…Н	H···N/N···H	H···Cl/Cl···H	HO/OH	H···C/C···H	C···C	Cl···O/O···Cl
Chrysene-DDQ	22.6	16.8	14.3	12.5	8.5	9.4	2.7
Benz(a)anthracene-DDQ	18.9	17.8	14.4	10.4	15.7	6.0	0.5
Triphenylene-DDQ	17.2	18.6	18.2	14.8	6.9	12.1	0.3
Benz(a)pyrene-DDQ	21.4	19.4	15.4	13.0	8.5	12.9	1.5
Dibenz[a,c]anthracene-DDQ	20.2	18.0	12.9	11.9	17.1	8.8	0.8
9H-Carbazole-DDQ	15.4	21.6	16.1	14.3	6.0	11.3	3.9
Range	15.4-22.6	16.8-21.6	12.9-18.2	10.4-14.3	6.0 - 17.1	6.0-12.9	0.3-3.9
Δ	7.2	4.8	5.3	3.9	11.1	6.9	3.6

while C···C interatomic contacts that prove the occurrence of the $\pi-\pi$ contacts between adjacent entities within the investigated crystals range from 6.0% in benz(a)anthracene-DDQ up to 12.9% in benz(a)pyrene-DDQ co-crystal. In accordance with the crystallographic data, the largest contributions of Cl···O interactions of 2.7% and 3.9% were registered in co-crystals chrysene-DDQ with DDQ association in centrosymmetric dimer, and 9H-carbazole-DDQ with DDQ homomeric helical chain in the co-crystal.

2.5. Degree of charge-transfer

Degree of charge-transfer in a specific co-crystal can be estimated from the geometry (bond lengths) of acceptor molecule in the co-crystal using the model proposed by Kistenmacher et al. for TCNQ acceptor using selected bond lengths [46-48]. The main idea of this model is that the negative charge on the TCNQ molecule results in delocalization of the quinoid structure. The more pronounced quinoid TCNQ structure corresponds to a smaller charge transfer, while the additional negative charge results in a lengthening of the shorter quinoid bonds and shortening of the remaining bond. As a characteristic of quinoid character of the molecule, ratio of sum of double bonds (a + e + f) to single bonds lengths (b + c + g + h) was chosen (Scheme 1). This approach gives decent agreement between experimental charge transfer and evaluated from this model data [49]. The same approach can be applied to the other acceptor molecules that have a quinoid structure, e.g. DDQ. Selected bonds of the DDQ molecule are shown in Scheme 1. Corresponding bond lengths of the optimized DDQ molecule and such molecules in different crystals are listed in Table 5. The cal-

$$\begin{array}{c|c}
C & O & O \\
C & O & O \\
C & O & O
\end{array}$$

$$\begin{array}{c|c}
C & O & O \\
C & O & O \\
C & O & O
\end{array}$$

$$\begin{array}{c|c}
C & O & O \\
C & O & O
\end{array}$$

$$\begin{array}{c|c}
C & O & O \\
C & O & O
\end{array}$$

$$\begin{array}{c|c}
C & O & O \\
C & O & O
\end{array}$$

$$\begin{array}{c|c}
C & O & O \\
C & O & O
\end{array}$$

Scheme 1. Notation of bonds for quinoid and aromatic configurations of DDQ.

culated ratio in all co-crystals is very close to the value in neutral DDQ, indicating that the CT is relatively weak.

3. Experimental

3.1. Materials

All materials used for cocrystallization have been purchased from Sigma-Aldrich and used without purification. Anhydrous solvents were obtained from the same company.

3.2. Synthesis of co-crystals

Initially co-crystals of all materials were crystallized by slow evaporation from dichloromethane solutions, but this method did not produce single crystals of sufficient quality for structure determination. Co-crystals satisfactory for X-ray study for all materials were obtained using vapor diffusion technique. For both compo-

Table 5Selected bond lengths of the DDQ molecules in the crystal, co-crystals and in the optimized molecule (gas phase).

Compound	a	b	с	d	e	f	g	h	(a+e+f) / (b+c+g+h)
DDQ gas phase (DFT)	1.207	1.505	1.424	1.154	1.355	1.352	1.717	1.495	0.637
DDQ [57]	1.2060(6)	1.4910(5)	1.4409(5)	1.1334(4)	1.3433(7)	1.3396(6)	1.6984(6)	1.4837(6)	0.636
Chrysene-DDQ	1.214(12)	1.475(12)	1.436(15)	1.145(14)	1.358(13)	1.356(14)	1.695(8)	1.468(15)	0.647
Benz(a)anthracene-DDQ	1.212(2)	1.487(2)	1.444(2)	1.125(3)	1.353(2)	1.349(3)	1.7061(17)	1.479(2)	0.639
Triphenylene-DDQ	1.222(10)	1.499(12)	1.453(11)	1.160(11)	1.344(11)	1.348(10)	1.694(7)	1.483(9)	0.639
Benzo(a)pyrene-DDQ	1.199(7)	1.502(7)	1.430(5)	1.135(5)	1.343(7)	1.340(6)	1.694(6)	1.482(5)	0.636
Dibenz[a , c]anthracene-DDQ	1.19(2)	1.47(2)	1.47(3)	1.14(2)	1.35(2)	1.36(2)	1.70(2)	1.48(2)	0.637
9H-Carbazole-DDQ	1.206(4)	1.494(5)	1.438(5)	1.144(5)	1.341(5)	1.343(5)	1.699(4)	1.483(5)	0.636

nents saturated solutions in chloroform were prepared. These solutions with molar ratio of co-formers 1:1 were mixed and filtered. After that they were placed in growth chamber of diffusion vessel, where they were exposed to rich atmosphere of pentane. If necessary, additional amount of pentane was added to the system. Usually, after 5–7 days elongated co-crystals with color different from initial reagents have been formed.

3.3. Computations

The HOMO and LUMO energies for each molecule were calculated with DFT using GAUSSIAN 16 software with B3LYP level of theory and 6-311+G(d,p) basis set [40]. The Hirshfeld surfaces are mapped with dnorm, and 2D fingerprint plots presented in this paper were generated using CrystalExplorer 2.1 [44,45].

3.4. X-ray crystallography

The single crystal X-ray data were collected from the very thin needle crystals (Table 3), the best crystals were selected from the repeated trials. X-ray data were obtained on a Bruker SMART APEXII CCD diffractometer (graphite monochromated Mo Klpha radiation, $\lambda = 0.71073$ Å, ω scans with a 0.5° step in ω) and Bruker D8 VENTURE diffractometer with microfocus seal tube [50]. Absorption corrections were applied by using the semiempirical method of the SADABS program [51]. The systematic absences in the diffraction data were consistent for the stated space groups. Co-crystals with benz(a)pyrene, dibez(a,c)anthracene and triphenylene were weakly diffracted as indicated by the low ratio of observed/unique reflections. The attempts to resolve the twinning for chrysene-DDQ co-crystal were unsuccessful. Despite the relatively high final R-values for these crystals, structure solution did not meet any difficulties and final structures look unambiguous. The structures were solved with Olex2 [52] and refined by full-matrix least-squares methods on F^2 with SHELXL [53] program package in anisotropic approximation for all non-hydrogen atoms. Hydrogen atoms were constrained to ride on their parent atoms with C-H = 0.95 Å and Uiso=1.2Ueq(C). In co-crystal benz(a)pyrene-DDQ the DDQ molecule is disordered by rotation of 180° about the central O = C...C = O axis with 60% to 40% ratio between disordered components (see Figure S2,d). Same type of disorder was found before in relative quinoid derivatives [54]. The carbazole in the carbazole-DDQ co-crystal was found disordered by two positions with occupancy factor 0.5 (Figure S2, f). The phenyl rings were refined as rigid groups. Figures were produced using MERCURY [55], molecular geometries were calculated using PLATON [56]. Figures S2d and S2f present position of DDQ(d) and carbazole (f) with and without disorder.

4. Conclusion

Six PAHs, chrysene, benz(a)anthracene, benz(a)pyrene, triphenylene, dibenz[*a,c*]anthracene and 9H-carbazole form 1:1 co-crystals

with DDQ acceptor. While the robust π - π interactions mediate mixed stacks as the primary structural motif of all the co-crystals, the auxiliary hydrogen bonds contribute significantly and provide some variations to the overall crystal packing of co-crystals. Among all six co-crystals, co-crystals chrysene-DDQ and carbazole-DDQ have the highest crystal densities and the most suitable packing with the shortest DDQ···DDQ contacts for both and D···D short contacts for chrysene and may consider for further study as potential OSCs with ambipolar and possible continuous p- (or n-) transport channels.

Declaration of Competing Interest

The authors declare that they have no known competing financial interests or personal relationships that could have appeared to influence the work reported in this paper.

Data availability

Data will be made available on request.

Acknowledgements

Authors are grateful to NSF for support via PREM grants DMR #1523611 and #2122108; MSF thanks the project ANCD 20.80009.5007.15 for support.

Supplementary materials

CCDC 2,129,413–2,129,418 contains the supplementary crystallographic data for six reported co-crystals. These data can be obtained free of charge via http://www.ccdc.cam.ac.uk/conts/retrieving.html, or from the Cambridge Crystallographic Data centre, 12 Union Road, Cambridge CB2 1EZ, UK; fax: (+44) 1223–336–033; or e-mail: deposit@ccdc.cam.ac.uk,

Supplementary material associated with this article can be found, in the online version, at doi:10.1016/j.molstruc.2023.134900.

References

- J. Ferraris, D.O. Cowan, V. Walatka, J.H. Perlstein, Electron transfer in a new highly conducting donor-acceptor complex, J. Am. Chem. Soc. 95 (1973) 948– 949, doi:10.1021/ja00784a066.
- [2] L.B. Coleman, M.J. Cohen, D.J. Sandman, F.G. Yamagishi, A.F. Garito, A.J. Heeger, Superconducting fluctuations and the peierls instability in an organic solid, Solid State Commun. 12 (1973) 1125–1132, doi:10.1016/0038-1098(73)90127-0.
- [3] S.R. Forrest, M.E. Thompson, Introduction: Organic Electronics and Optoelectronics, Chem. Rev. 107 (2007) 923–925, doi:10.1021/cr0501590.
- [4] W. Zhu, R. Zheng, X. Fu, H. Fu, Q. Shi, Y. Zhen, H. Dong, W. Hu, Revealing the charge-transfer interactions in self-assembled organic cocrystals: two-dimensional photonic applications, Angew. Chem. Int. Ed. 127 (2015) 6889–6893, doi:10.1002/anie.201501414.
- [5] J. Zhang, J. Jin, H. Xu, Q. Zhang, W. Huang, Recent progress on organic donoracceptor complexes as active elements in organic field-effect transistors, J. Mat. Chem. C. 6 (2018) 3485–3498, doi:10.1039/C7TC04389A.

- [6] T. Hasegawa, K. Mattenberger, J. Takeya, B. Batlogg, Ambipolar field-effect carrier injections in organic Mott insulators, Phys. Rev. B 69 (2004) 245115.
- [7] Y. Qin, J. Zhang, X. Zheng, H. Geng, G. Zhao, W. Xu W. Hu, Z. Shuai, D. Zhu, Charge-Transfer Complex Crystal Based on Extended-π-Conjugated Acceptor and Sulfur-Bridged Annulene: Charge-Transfer Interaction and Remarkable High Ambipolar Transport Characteristics, Adv. Mater. 26 (2014) 4093– 4000
- [8] Y.K. Qin, C.L. Cheng, H. Geng, C. Wang, W.P. Hu, W. Xu, Z.G. Shuai, D.B. Zhu, Efficient ambipolar transport properties in alternate stacking donor-acceptor complexes: from experiment to theory, Phys. Chem. Chem. Phys. 18 (2016) 14094.
- [9] L.Y. Zhu, Y.P. Yi, Y. Li, E.G. Kim, V. Coropceanu, J.L. Brédas, Prediction of Remarkable Ambipolar Charge-Transport Characteristics in Organic Mixed-Stack Charge-Transfer Crystals, J. Am. Chem. Soc. 134 (2012) 2340–2347.
- [10] L. Zhu, Y. Yi, A. Fonari, N.S. Corbin, V. Coropceanu, J.-.L. Brédas, Electronic Properties of Mixed-Stack Organic Charge-Transfer Crystals, J. Phys. Chem. C 118 (2014) 14150–14156, doi:10.1021/jp502411u.
- [11] A. Mandal, A. Choudhury, S. Sau, P.K. Iyer, P. Mal, Exploring Ambipolar Semi-conductor Nature of Binary and Ternary Charge-Transfer Cocrystals of Triphenylene, Pyrene, and TCNQ, J. Phys. Chem. C 124 (2020) 6544–6553, doi:10.1021/acs.jpcc.0c00426.
- [12] T. Salzillo, M. Masino, G. Kociok-Köhn, D. Di Nuzzo, E. Venuti, R.G. Della Valle, D. Vanossi, C. Fontanesi, A. Girlando, A. Brillante, E. Da Como, Structure, Stoichiometry, and Charge Transfer in Cocrystals of Perylene with TCNQ-FxCryst, Growth Des. 16 (2016) 3028–3036, doi:10.1021/acs.cgd.5b01663.
- [13] D. Vermeulen, L.Y. Zhu, K.P. Goetz, P. Hu, H. Jiang, C.S. Day, O.D. Jurchescu, V. Coropceanu, C. Kloc, L.E. McNeil, Charge Transport Properties of Perylene–TCNQ Crystals: The Effect of Stoichiometry, J. Phys. Chem. C 118 (2014) 24688–24696, doi:10.1021/jp508520x.
- [14] K.P. Goetz, J.Y. Tsutsumi, S. Pookpanratana, J. Chen, N.S. Corbin, R.K. Behera, V. Coropceanu, C.A. Richter, C.A. Hacker, T. Hasegawa, O.D. Jurchescu, Polymorphism in the 1:1 Charge-Transfer Complex DBTTF-TCNQ and Its Effects on Optical and Electronic Properties, Adv. Electron. Mater. 2 (2016) 16002031–160020310
- [15] Q. Ai, Y.A. Getmanenko, K. Jarolimek, R. Castañeda, T.V. Timofeeva, C. Risko, Unusual Electronic Structure of the Donor-Acceptor Cocrystal Formed by Dithieno[3,2-a:2',3'-c]phenazine and 7,7,8,8-Tetracyanoquinodimethane, J. Phys. Chem. Lett. 8 (2017) 4510–4515, doi:10.1021/acs.jpclett.7b01816.
- [16] L. Sun, Y. Wang, F. Yang, X. Zhang, W. Hu, Cocrystal Engineering: A Collaborative Strategy toward Functional Materials, Adv. Mater. (2019) 1902328, doi:10.1002/adma.201902328.
- [17] H. Jiang, P. Hu, J. Ye, K.K. Zhang, Y. Long, W. Hu, C. Kloc, Tuning of the Degree of Charge Transfer and Electronic Properties in Organic Binary Compounds by Crystal Engineering: A Perspective, J. Mat Chem. C 6 (2018) 1884–1902, doi:10. 1039/C7TC049821.
- [18] V. Gude, K. Biradha, Effect of Noncovalent Interactions on the Intersystem Crossing Behavior in Charge-Transfer Cocrystals of 3,5-Dinitrobromobenzene, J. Phys. Chem. C 125 (2021) 120–129, doi:10.1021/acs.jpcc.0c08726.
- [19] Y. Aoyama, K. Endo, T. Anzai, Y. Yamaguchi, T. Sawaki, K. Kobayashi, N. Kanehisa, H. Hashimoto, Y. Kai, H. Masuda, Crystal Engineering of Stacked Aromatic Columns. Three-Dimensional Control of the Alignment of Orthogonal Aromatic Triads and Guest Quinones via Self-Assembly of Hydrogen-Bonded Networks, J. Am. Chem. Soc. 118 (24) (1996) 5562–5571, doi:10.1021/jij953800k
- [20] N. Yee, A. Dadvand, E. Hamzehpoor, H.M. Titi, D.F. Perepichka, Hydrogen Bonding Versus πStacking in Charge-Transfer Co-crystals, Cryst. Growth Des. 21 (5) (2021) 2609–2613, doi:10.1021/acs.cgd.1c00309.
- [21] N.R. Goud, A.J. Matzger, -Impact of hydrogen and halogen bonding interactions on the packing and ionicity of charge-transfer cocrystals, Cryst. Growth Des. 17 (2017) 328–336, doi:10.1021/acs.cgd.6b01548.
- [22] J.J. Mayerle, J.B. Torrance, The design of organic metals dibenzotetrathia-fulvalene-2,3-dichloro-5,6-dicyano-p-benzoquinone (DBTTF-DDQ), Bull. Chem. Soc. Jpn. 54 (1981) 3170–3172.
- [23] S. Mohamud, V. Phuoc, L. del Campo, N.E. Massa, S. Pagola, TTF-DDQ: two "green" synthetic routes, crystal structure and band gap from FT-IR spectroscopy, Synth. Met. 214 (2016) 71 https://www.elsevier.com/open-access/ userlicense/1.0/.
- [24] U. Behrens, R.D. Calleja, M. Dotze, U. Franke, W. GunDer, G. Klar, J. Kudnig, F. Olbrich, E.S. Martinez, M.J. Sanchis, B. Zimmer, Structure, dielectric relaxation and electrical conductivity of 2,3,7,8-tetramethoxychalcogenanthrene-2,3-dichloro-5,6-dicyano-1,4-benzoquinone 1: 1 charge-transfer complexes, J. Mater. Chem. 6 (1996) 547–553.
- [25] E. Gebert, A.H. Reis, J.S. Miller, H. Rommelmann, A.J. Epstein, Characterization of the 1: 1 charge-transfer reaction between decamethylferrocene and 2,3-dichloro-5,6-dicyanoquinone (DDQ): Structure of the DDQH- Anion, J. Am. Chem. Soc. 104 (1982) 4403–4410, doi:10.1021/ja00380a015.
- [26] J.C. Zhong, M. Maekawa, T. Kuroda-Sowa, Yu. Suenaga, T. Ohta, M. Munakata, Crystal Structure of 1:1 Donor-Acceptor Complex between 9,10-Benzophenanthrene and 2,3,5,6,-Tetrafluoro-1,4-benzoquinone, Analyt. Sci. 18 (2002) 851–852.
- [27] K. Prout, I.J. Tickle, Molecular Complexes. Part XX11.1 Crystal and Molecular Structure of the Molecular Complex of Pyrene and Chloranil Chemical Crystallography Laboratory, Oxford University, South Parks
- [28] A.W. Hanson, The Crystal Structure of the 1:1 Perylene-Fluoranil Complex, Acta Crystallogr. 16 (1963) 1147-.

- [29] B. Shaanan, U. Shmueli, M. Colapietro, Structure and Packing Arrangement of Molecular Compounds. X. 9,10-Diazaphenanthrene-2,3-Dichloro-5,6dicyano-1,4-benzoquinone (2:1), Acta Cryst. B38 (1982) 818–824, doi:10.1107/ S0567740882004142.
- [30] J. Bernstein, H. Regev, F.H. Herbstein, Molecular compounds and complexes. X. The crystal structure of the π-molecular compound benzo[c]phenanthrene-2,3-dichloro-5,6-dicyanobenzoquinone, Acta Crystallogr. B33 (1977) 1716–1724, doi:10.1107/S0567740877006943.
- [31] F.H. Herbstein, M. Kapon, G. Rzonzew, D. Rabinovich, Molecular Compounds and Complexes. XI.* The Crystal Structure of the N-Molecular Compound Phenanthrene-2,3-Dichloro-5,6-dicyano-p-benzoquinone, Acta Cryst. B34 (1978) 476–481.
- [32] P.J. Munnoch, J.D. Wright, Crystal Structure of the 1:1 Molecular Complex of Chrysene and Tetrafluoro-p-benzoquinone (Fluoranil), J.C.S. Perkin II (1975) 1071–1074
- [33] R.A. Wiscons, V. Coropceanu, A.J. Matzger, Quaternary Charge-Transfer Solid Solutions: Electronic Tunability through Stoichiometry, Chem. Mater. 31 (2019) 6598–6604, doi:10.1021/acs.chemmater.9b00502.
- [34] R.K. Behera, N.R. Goud, A.J. Matzger, J.-.L. Brédas, V. Coropceanu, Electronic Properties of 1,5-Diaminonaphthalene: Tetrahalo-1,4-benzoquinone Donor-Acceptor Cocrystals, J. Phys. Chem. C 121 (2017) 23633–23641, doi:10.1021/acs.jpcc.7b08360.
- [35] K. Molčanov, D. Štalke, A. Šantić, S. Demeshko, V. Stilinović, Z. Mou, M. Kertesz, B. Kojić-Prodić, Probing semiconductivity in crystals of stable semiquinone radicals: organic salts of 5,6-dichloro-2,3-dicyanosemiquinone (DDQ) radical anion, CrystEngComm 20 (2018) 1862–1873, doi:10.1039/C7CE02146A.
- [36] K. Thakur, D. Wang, S.V. Lindeman, R. Rathore, A synthesis of doubly-annulated m-terphenyl based molecular tweezers and their charge-transfer complexes with DDQ as a guest, Chem. Eur. J. 24 (2018) 13106–13109, doi:10.1002/chem. 201803137.
- [37] R.R. Dasari, X. Wang, R.A. Wiscons, H.F. Haneef, A. Ashokan, Y. Zhang, M.S. Fonari, S. Barlow, V. Coropceanu, T.V. Timofeeva, O.D. Jurchescu, J.-L. Brédas, A.J. Matzger, S.R. Marder, Charge-Transport Properties of F6TNAP-Based Charge-Transfer Cocrystals, Adv. Funct. Mat. 29 (2019) 1904858, doi:10.1002/ adfm.201904858.
- [38] J. Harada, N. Yoneyama, S. Sato, Y. Takahashi, T. Inabe, Crystals of Charge-Transfer Complexes with Reorienting Polar Molecules: Dielectric Properties and Order-Disorder Phase Transitions Cryst, Growth Des. 19 (2019) 291–299, doi:10.1021/acs.cgd.8b01418.
- [39] A. Sygula, M. Yanney, W.P. Henry, F.R. Fronczek, A.V. Zabula, M.A. Petrukhina, Cryst. Growth Des. 14 (2014) 2633.
- [40] Gaussian 16, Revision B.01, M.J. Frisch, G.W. Trucks, H.B. Schlegel, G.E. Scuseria, M.A. Robb, J.R. Cheeseman, G. Scalmani, V. Barone, G.A. Petersson, H. Nakatsuji, X. Li, M. Caricato, A.V. Marenich, J. Bloino, B.G. Janesko, R. Gomperts, B. Mennucci, H.P. Hratchian, J.V. Ortiz, A.F. Izmaylov, J.L. Sonnenberg, D. Williams-Young, F. Ding, F. Lipparini, F. Egidi, J. Goings, B. Peng, A. Petrone, T. Henderson, D. Ranasinghe, V.G. Zakrzewski, J. Gao, N. Rega, G. Zheng, W. Liang, M. Hada, M. Ehara, K. Toyota, R. Fukuda, J. Hasegawa, M. Ishida, T. Nakajima, Y. Honda, O. Kitao, H. Nakai, T. Vreven, K. Throssell, J.A. Montgomery, Jr., J.E. Peralta, F. Ogliaro, M.J. Bearpark, J.J. Heyd, E.N. Brothers, K.N. Kudin, V.N. Staroverov, T.A. Keith, R. Kobayashi, J. Normand, K. Raghavachari, A.P. Rendell, J.C. Burant, S.S. Iyengar, J. Tomasi, M. Cossi, J.M. Millam, M. Klene, C. Adamo, R. Cammi, J.W. Ochterski, R.L. Martin, K. Morokuma, O. Farkas, J.B. Foresman, D.J. Fox, Gaussian, Inc., Wallingford CT, 2016.
- [41] Y. Nakagawa, Y. Takahashi, J. Harada, T. Inabe, The bis(ethylenedithio)tetrathiafulvalene-based ionic charge-transfer complex with 2,3-dichloro-5,6-dicyano-p-benzoquinone, Acta Cryst. C69 (2013) 400– 402, doi:10.1107/S0108270113003685.
- [42] G.R. Desiraju, A. Gavezzotti, Crystal structures of polynuclear aromatic hydrocarbons. Classification, rationalization and prediction from molecular structure, Acta Crystallogr. B45 (1989) 473–482.
- [43] V.R. Hathwar, M. Sist, Ma.R.V. Jørgensen, A.H. Mamakhel, X. Wang, C.M. Hoffmann, K. Sugimoto, J. Overgaard, B.B. Iversen, Quantitative analysis of intermolecular interactions in orthorhombic rubrene, IUCrJ 2 (2015) 563–574 http://dx.doi.org/10.1107/S2052252515012130.
- [44] J.J. McKinnon, M.A. Spackman, A.S. Mitchell, Acta Crystallogr. B60 (2004) 627–668.
- [45] S.K. Wolff, D.J. Grimwood, J.J. McKinnon, D. Jayatilaka, M.A. Spackman, Crystal-Explorer 2.1, University of Western Australia, Perth, Australia, 2007.
- [46] T.J. Kistenmacher, T.J. Emge, A.N. Bloch, D.O. Cowan, Structure of the red, semiconducting form of 4,4',5,5'-tetramethyl-[Delta]2, 2'-bi-1,3-diselenole-7,7,8,8-tetracyano-p-quinodimethane, TMTSF-TCNQ, Acta Crystallogr. B38 (1982) 1193–1199.
- [47] P. Coppens, T.N.G. Row, X-Ray Diffraction Measurement of Net Atomic and Molecular Charges, Ann. N. Y. Acad. Sci. 313 (1) (1978) 244–255.
- [48] S. Flandrois, D. Chasseau, Longueurs de liaison et transfert de charge dans les sels du tetracyanoquinodimethane (TCNQ), Acta Crystallogr. B33 (1977) 2744–2750
- [49] B. Averkiev, R. Isaac, E.V. Jucov, V.N. Khrustalev, C. Kloc, L.E. McNeil, T.V. Timofeeva, Evidence of Low-Temperature Phase Transition in Tetracene– Tetracyanoquinodimethane Complex, Cryst. Growth Des. 18 (2018) 4095–4102, doi:10.1021/acs.cgd.8b00501.
- [50] BrukerSAINT (Version 6.36a), Bruker-AXS Inc., Madison, Wisconsin, USA, 2002.
- [51] BrukerSMART (Version 5.625) and SADABS (Version 2.03a), Bruker AXS Inc., Madison, Wisconsin, USA, 2001.

- [52] O.V. Dolomanov, L.J. Bourhis, R.J. Gildea, J.A.K. Howard, H. Puschmann, J. Appl. Cryst. 42 (2009) 339–341.
 [53] G.M. Sheldrick, Acta Crystallogr. A64 (2008) 112–122.
 [54] K. Molčanov, V. Milašinović, B. Kojić-Prodić, Contribution of Different Crystal Packing Forces in π-Stacking: From Noncovalent to Covalent Multicentric Bonding, Cryst. Growth Des. 19 (2019) 5967–5980 http://dx.doi.org/10.1021/acs.cgd.9b00540.
- [55] C.F. Macrae, I.J. Bruno, J.A. Chisholm, P.R. Edgington, P. McCabe, E. Pidcock, L. Rodriguez-Monge, R. Taylor, J. van de Streek, P.A. Wood, Mercury CSD 2.0 new features for the visualization and investigation of crystal structures, J.
- Appl. Cryst. 41 (2008) 466–470, doi:10.1107/S0021889807067908. [56] A.L. Spek, PLATON, molecular geometry program, J. Appl. Crystallogr. 36 (2003) 7–13.
- [57] G. Zanotti, R. Bardi, A. Del Pra, Acta Cryst. B36 (1980) 168–171.